

AlN and AlScN RF Microsystems

Prof. Matteo Rinaldi

Director of Northeastern SMART Center

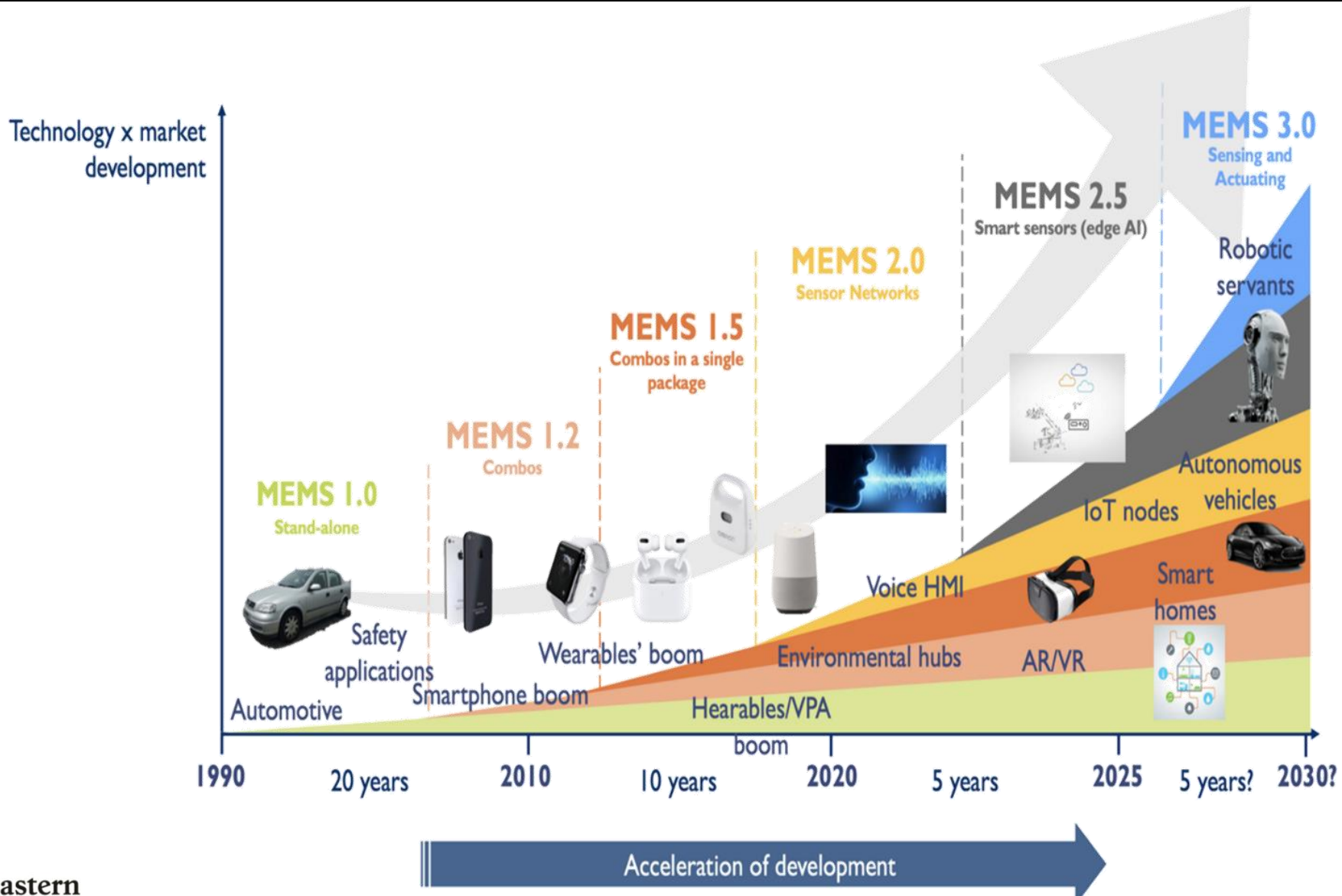
Northeastern University

Boston, MA 02115, USA

rinaldi@northeastern.edu

<https://youtu.be/UCS4x1OlQ4Y>

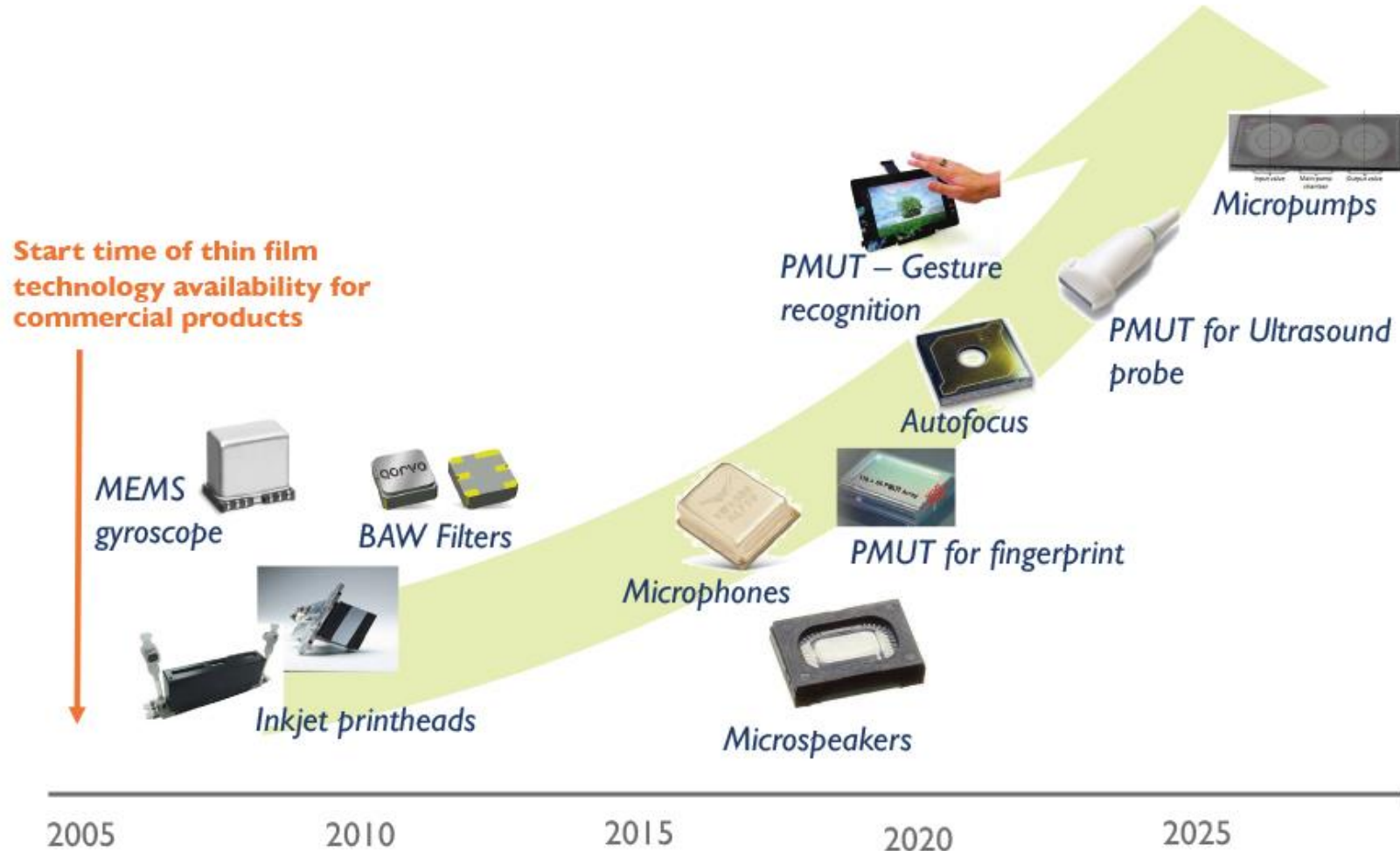
MEMS in Consumer Products



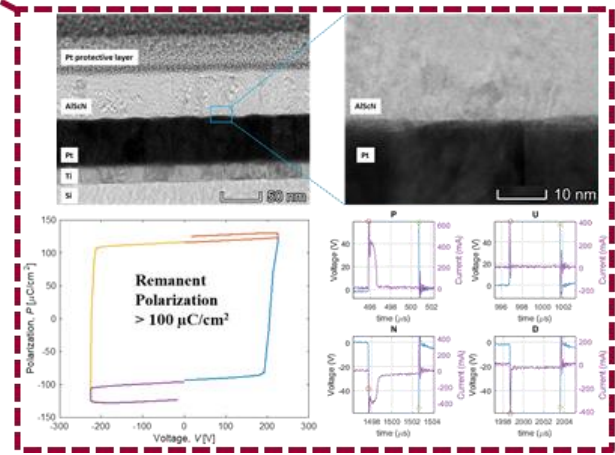
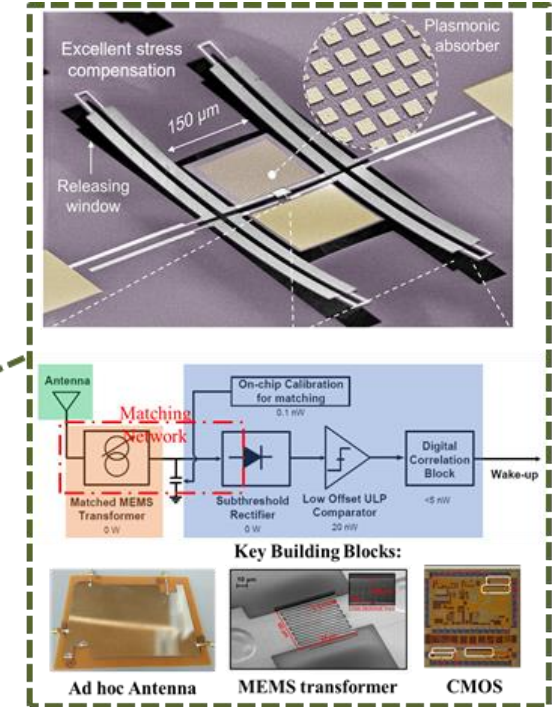
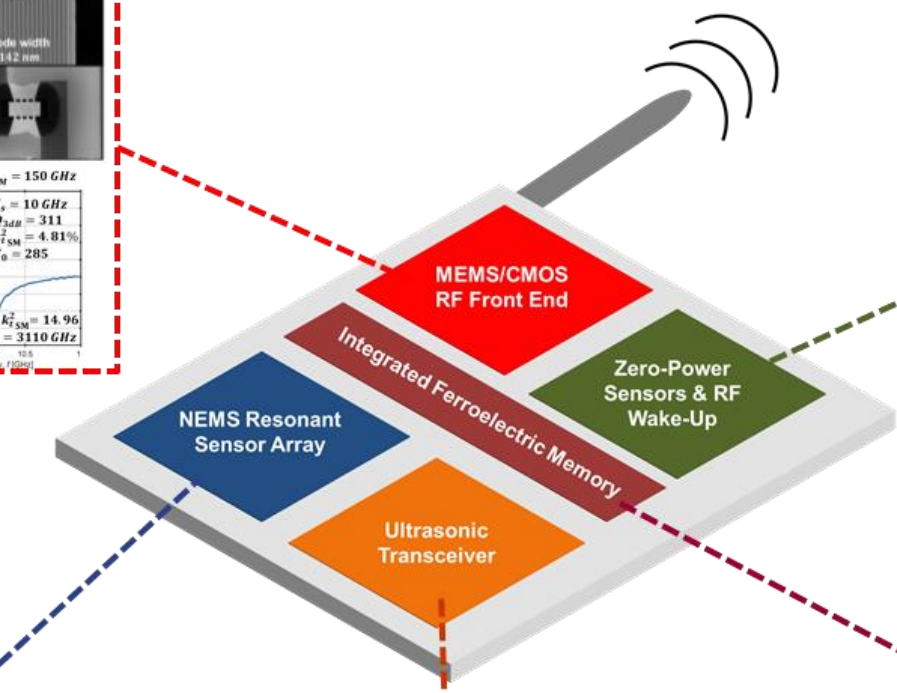
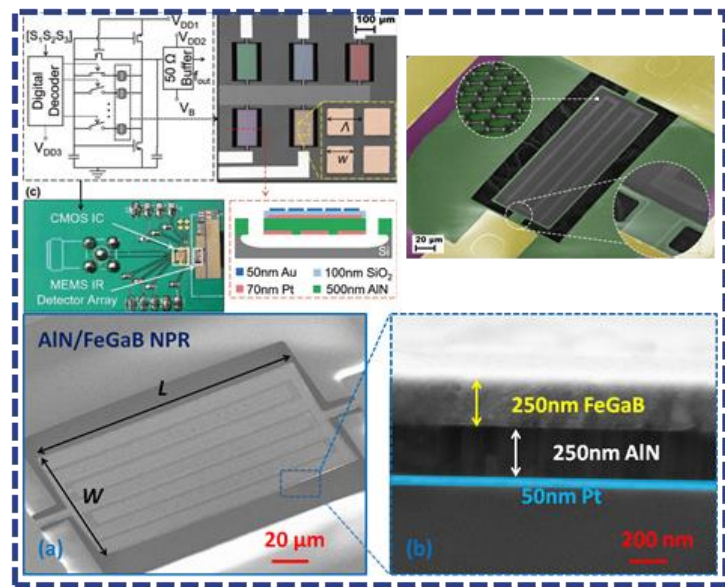
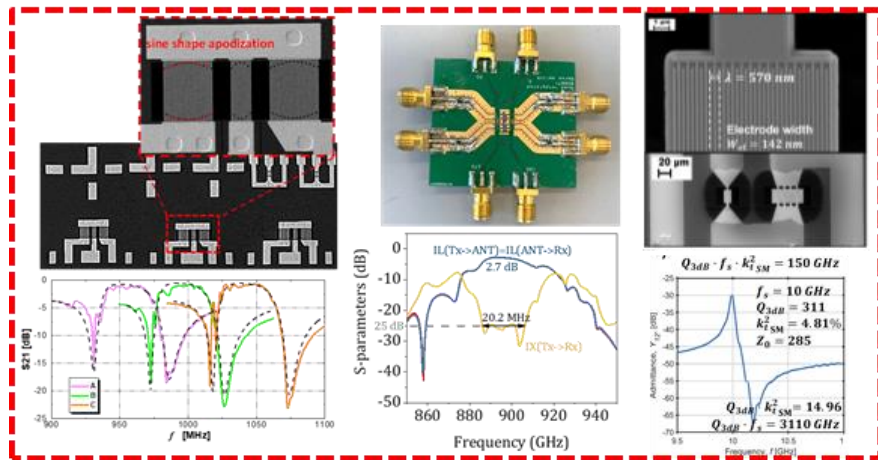
Piezo MEMS in Consumer Products

Piezo MEMS time to market: 2018-2025

(Source: Status of the MEMS Industry 2019, Yole Développement, June 2019)

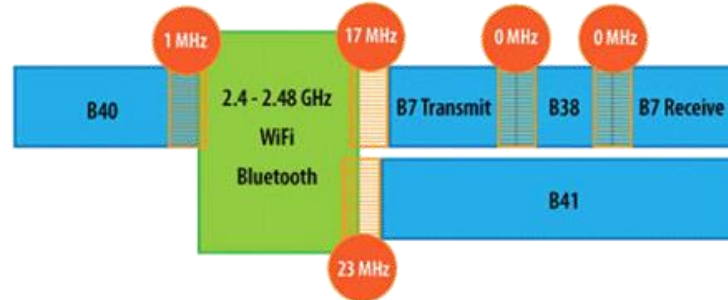


Multi-Functional and Near-Zero Power Piezo Microsystems



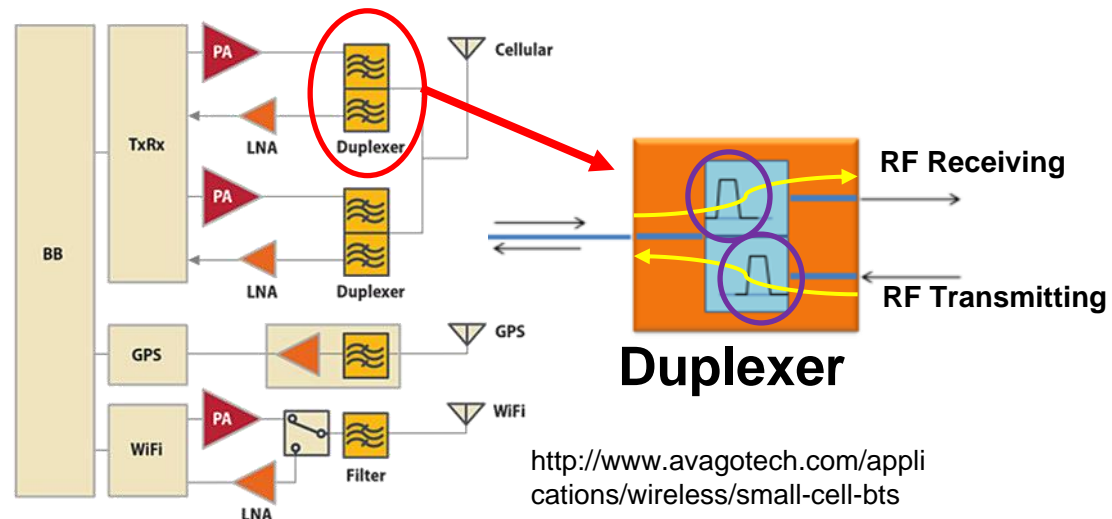
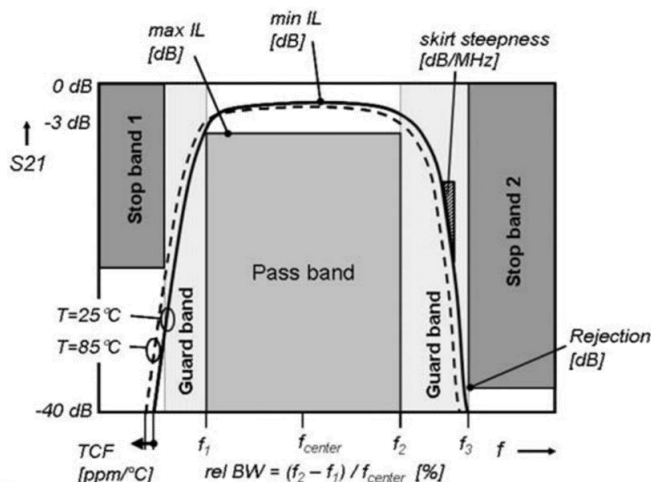
Radio Frequency Filters - Needs

- 4G/LTE frequency bands are often co-located next to other frequency bands with little to no guard band separating adjacent bands and have challenging TX/RX frequency separation



<http://www.avagotech.com/products/wireless/fbar/>

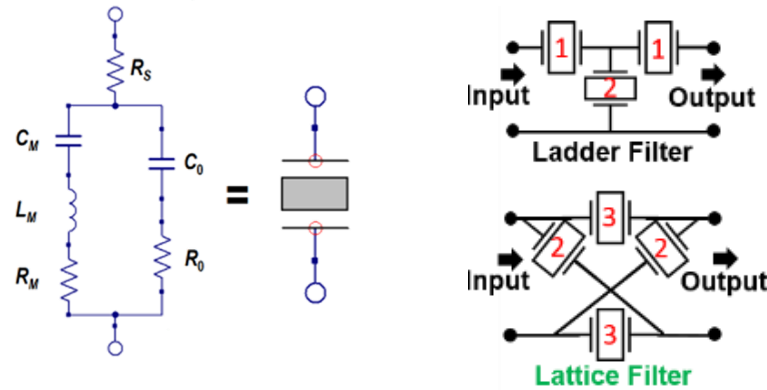
- Miniaturized RF filters with **low-loss, large skirt steepness** and **out of band rejection** are required to satisfy the 4G/LTE stringent **multi-band operation** requirements:



<http://www.avagotech.com/applications/wireless/small-cell-bts>

Microacoustic RF Filters

- Micro acoustic resonators guarantee high Q in a reduced form factor not achievable with LC networks
- Nth-order filters are formed by N micro-acoustic resonators electrically (or mechanically) coupled

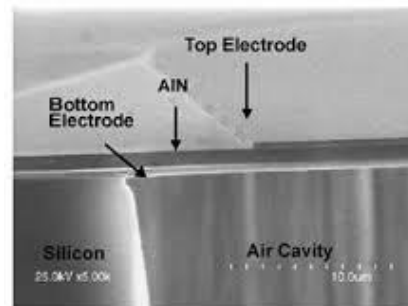
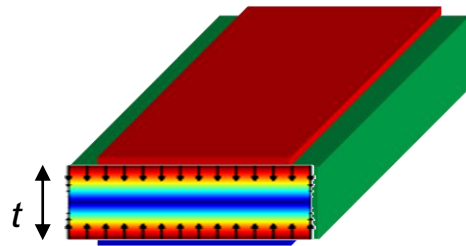


$$BW \propto k_t^2$$

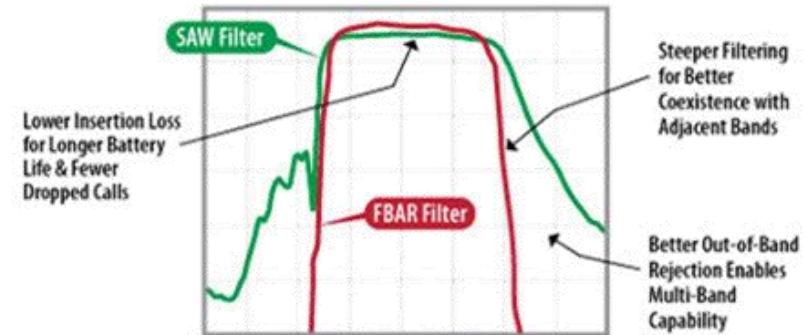
$$S.S \propto Q$$

$$I.L. \propto \frac{1}{Q \cdot k_t^2}$$

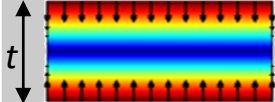
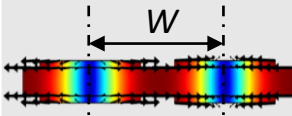
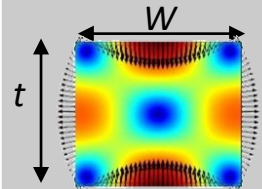
- Aluminum Nitride FBAR (Film Bulk Acoustic Resonator) has gone mainstream thanks to superior performance with steeper rejection curves compared to surface acoustic wave (SAW) filters



Ruby et al.



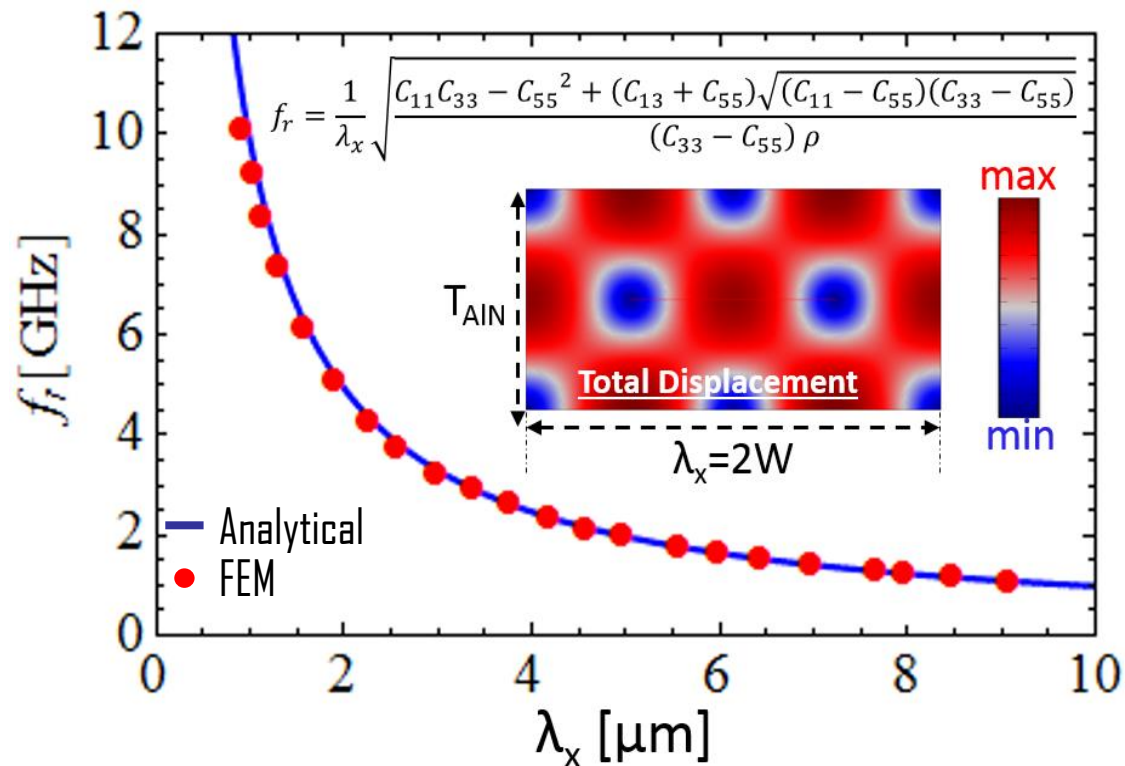
AlN Microacoustic RF Filters

| Technology | Mode Shape | f_0 | k_t^2 | Q | Frequency Tuning |
|--------------|--|--|---|-------------|--|
| <i>FBAR</i> |  | $\propto \frac{1}{T}$ | $\propto e_{33}^2 \approx 5\sim 7\%$ | 1000 ~ 5000 | <i>Non lithographic</i> |
| <i>CMR</i> |  | $\propto \frac{1}{W}$ | $\propto e_{31}^2 \approx 1\sim 2\%$ | 1000 ~ 5000 | <i>Lithographic (full range)</i> |
| <i>CLMR*</i> |  | $f_r \propto \frac{1}{T}, \frac{1}{W}$ | $\propto \frac{2}{\pi} (e_{31}^2 + e_{33}^2) \approx 5\sim 7\%$ | 1000 ~ 5000 | <i>Lithographic (40%, $k_t^2 \geq 5\%$)</i> |

* C. Cassella, et al., "Aluminum Nitride Cross-Sectional Lamé Mode Resonators," *J. Microelectromechanical Syst.*, pp. 1–11, 2016.

Cross-Sectional Lamé Mode Resonators

$$\begin{bmatrix} \mu_x \\ \mu_z \end{bmatrix} = \begin{bmatrix} A(x)B(z) \\ C(x)D(z) \end{bmatrix} = \begin{bmatrix} \cos(\beta_x x) \sin(\beta_z z) \\ -\sin(\beta_x x) \cos(\beta_z z) \end{bmatrix}$$



2-D Displacement vector

Lamé mode **exact** solution:

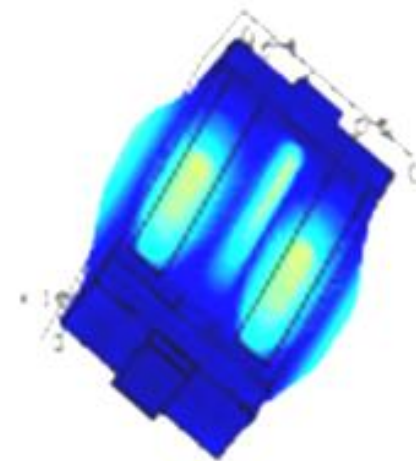
$$\frac{W}{T_{AIN}} = \sqrt{\frac{(C_{11} - C_{55})}{(C_{33} - C_{55})}} \sim 1$$

$$\mu_x^{peak} = \mu_z^{peak}$$

Lamé mode **degenerate** solutions:

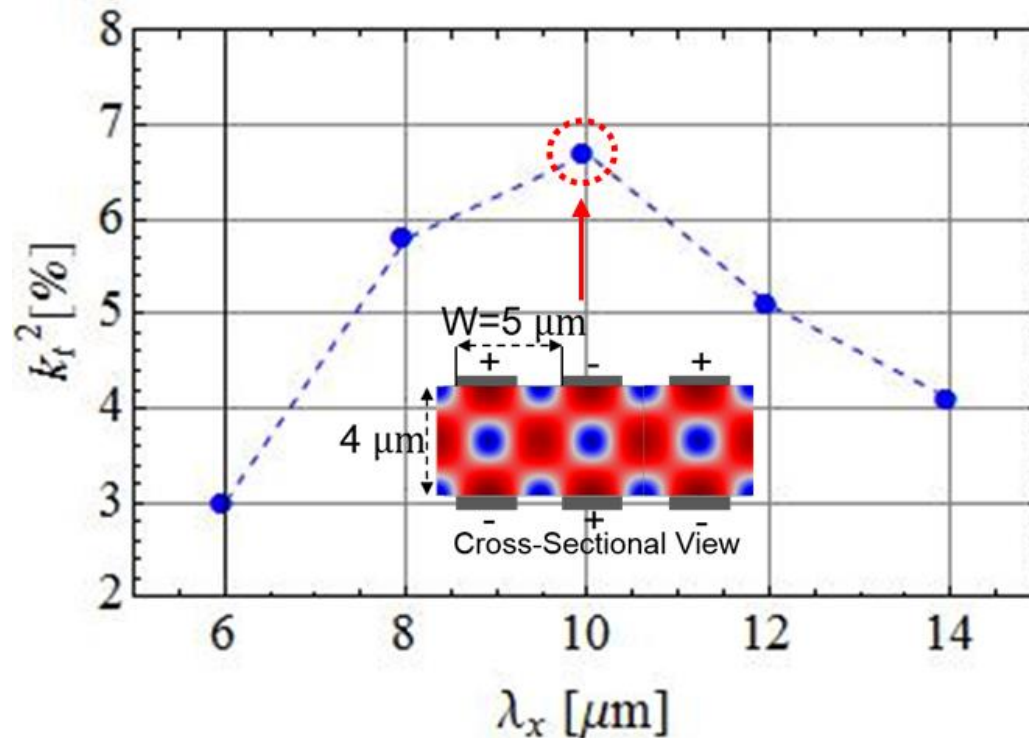
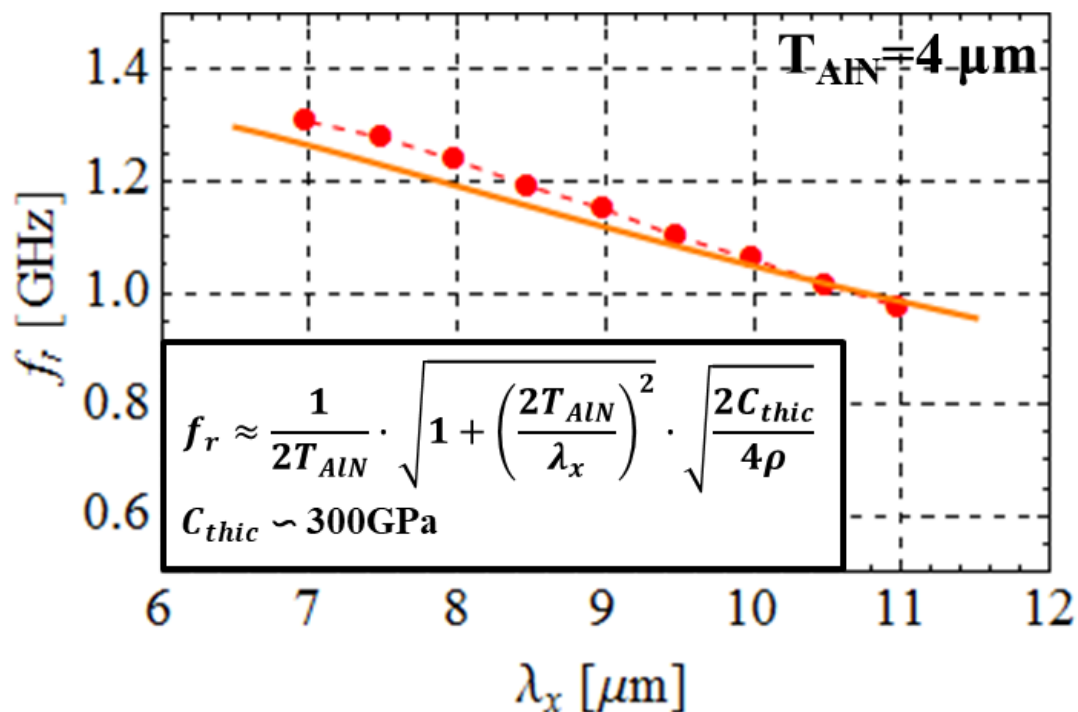
$$\frac{W}{T_{AIN}} \neq \sqrt{\frac{(C_{11}C_{55})}{(C_{33} - C_{55})}}$$

$C_{x,y}$ = Components of the AlN stiffness matrix



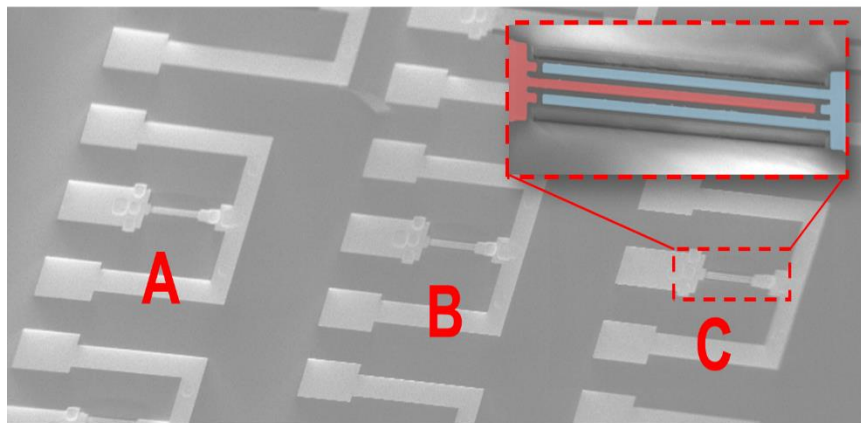
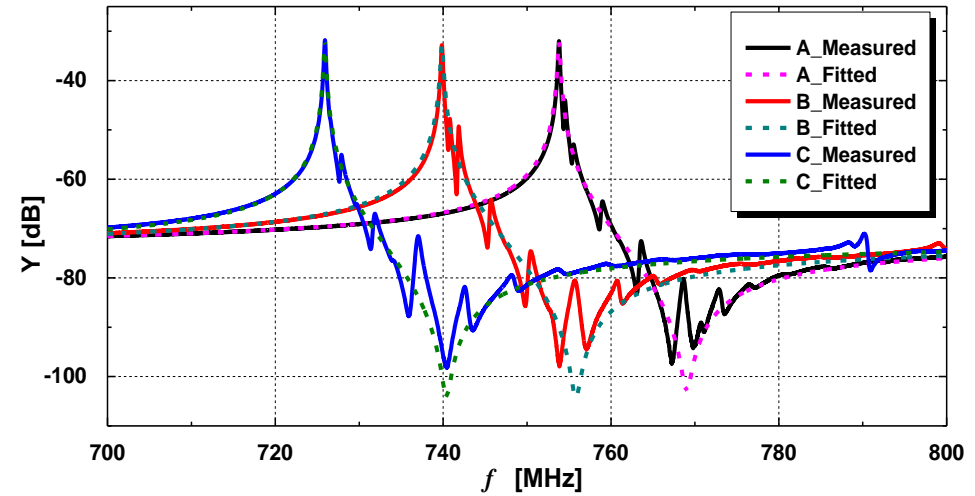
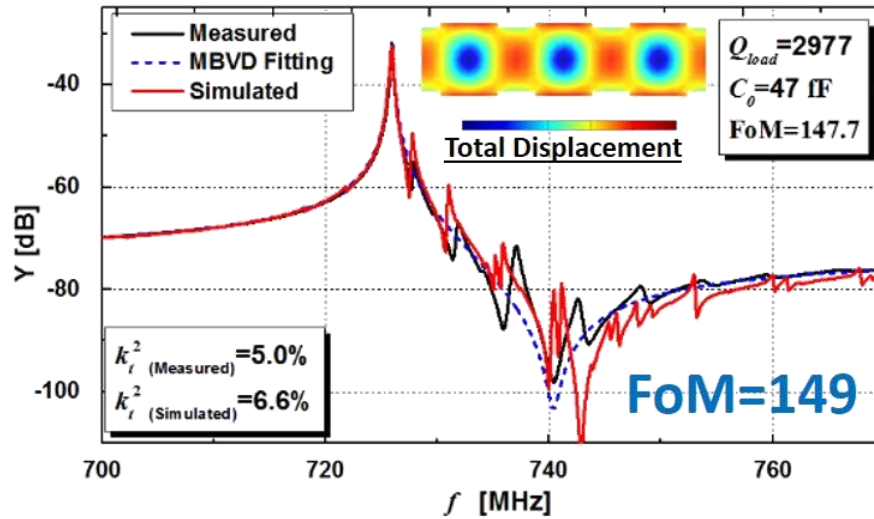
Cross-Sectional Lamé Mode Resonators

Degenerate CLM - $u_x^{peak} \neq u_z^{peak}$ but k_t^2 can be high-enough in a broad range of λ_x/T_{AIN}



>40% lithographic tuning with $k_t^2 \geq 5\%$

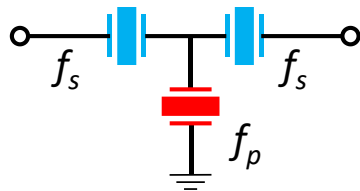
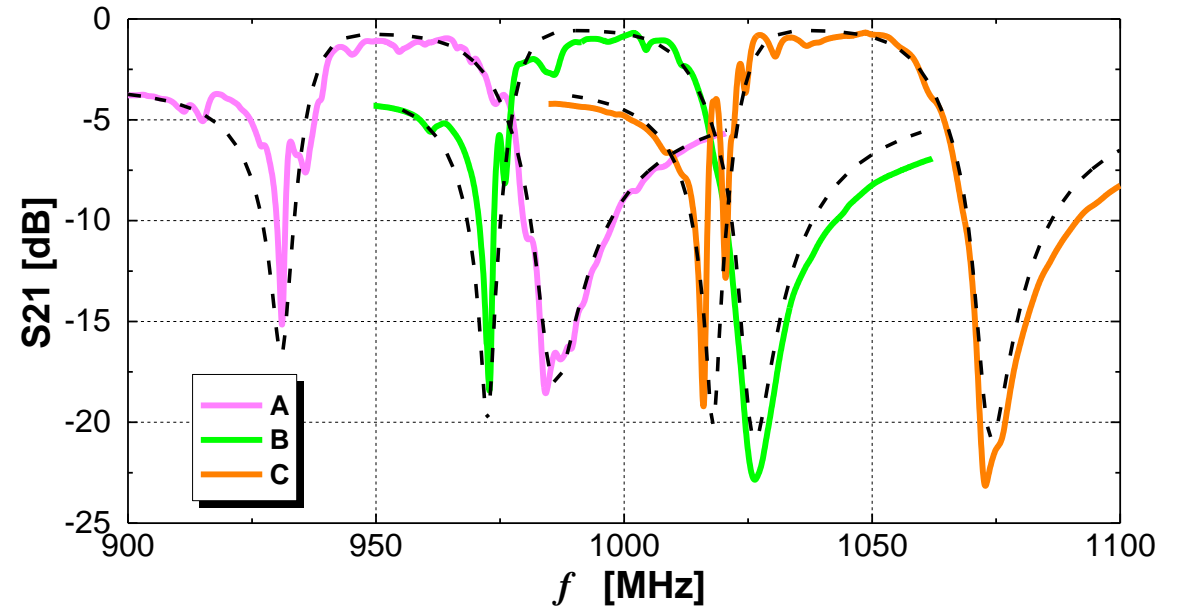
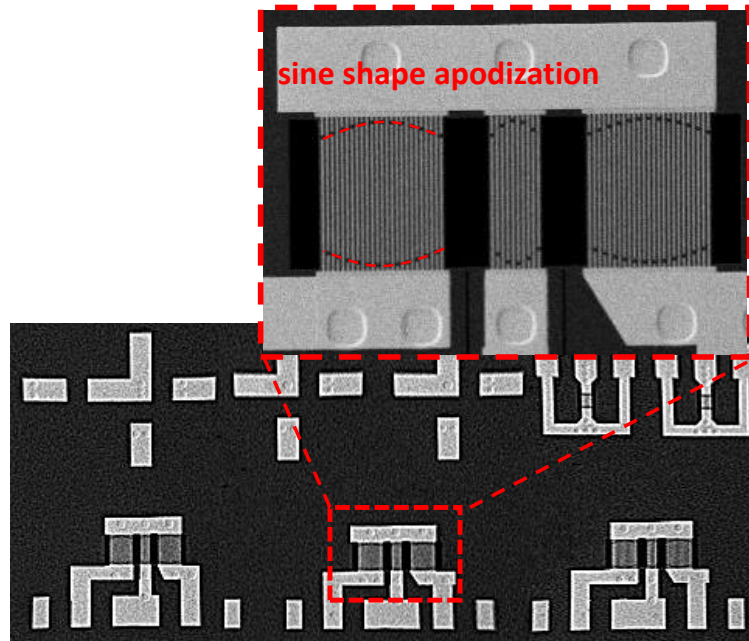
AlN Cross-Sectional Lamé Mode Resonators – Record FoM



| Device | Pitch [μm] | Q_{load} | k_t^2 | f_r [MHz] | FoM |
|--------|-------------------------|------------|---------|-------------|-------|
| A | 5.0 | 2820 | 5.0% | 753.8 | 141.0 |
| B | 5.2 | 2493 | 5.4% | 739.9 | 134.6 |
| C | 5.4 | 2977 | 5.0% | 725.9 | 147.7 |

AlN Cross-Sectional Lamé Mode Filters

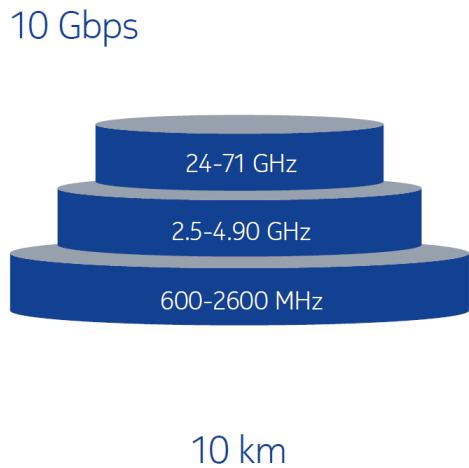
High fractional bandwidth ($BW > 3.9\%$) and unprecedented levels of loss ($IL < 1\text{dB}$) and *spurious suppression* enabled by the combined use of thicker platinum electrodes and **apodization techniques**



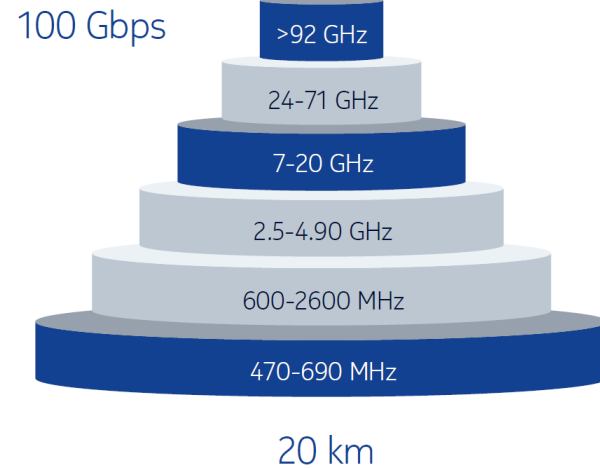
| Filter | Resonator | Pitch [μm] | Comsol Simulation | | Fitting | | Measurement | | |
|--------|-----------|-------------------------|-------------------------|---------|---------|------|-------------|------|--------------|
| | | | Static Capacitance [fF] | k_t^2 | k_t^2 | FBW | IL [dB] | FBW | Termination |
| A | Series | 4.9 | 358 | 7.6% | 6.5% | 3.9% | 0.9 | 4.0% | |
| | Parallel | 5.1 | 146 | 7.6% | | | | | |
| B | Series | 4.6 | 346 | 7.5% | 6.5% | 3.7% | 0.7 | 3.9% | 700 Ω |
| | Parallel | 4.8 | 141 | 7.4% | | | | | |
| C | Series | 4.3 | 334 | 7.1% | 6.5% | 3.8% | 0.7 | 4.0% | |
| | Parallel | 4.5 | 136 | 7.4% | | | | | |

New Paradigms and Opportunities for the 6G Spectrum

5G wedding cake



6G wedding cake



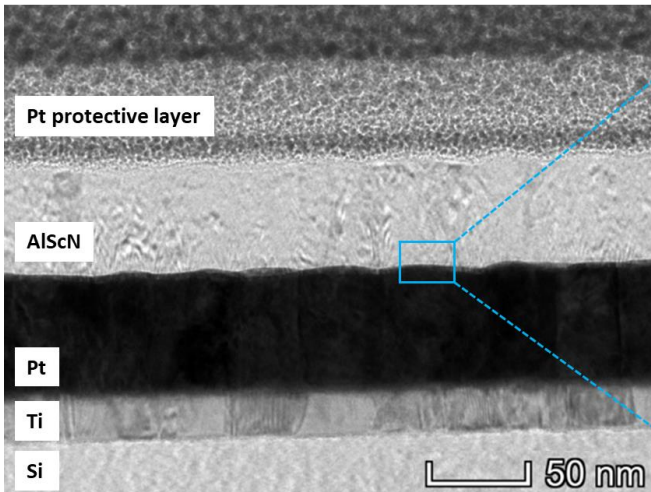
- Sensing and short range
- Hotspot capacity
- Urban extreme capacity
- Urban capacity
- Wide area coverage
- Extreme wide area IoT

| Resonator Metric | Low spectrum | Mid Spectrum |
|---------------------------------|--------------|--------------|
| Frequency | 470-690 MHz | 7-20 GHz |
| k_t^2 (~BW) | >10% | >4% |
| Q | >500 | >250 |

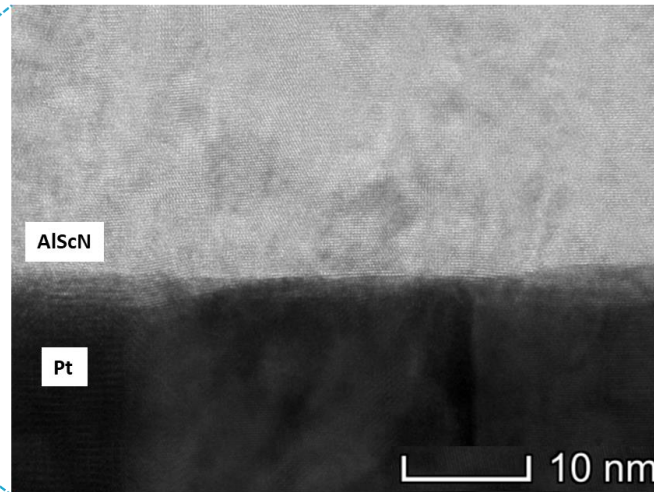
H. Holma, et al., "Extreme massive MIMO for macro cell capacity boost in 5G-Advanced and 6G." Nokia Bell Labs

Breakthroughs in resonator material and design highly needed

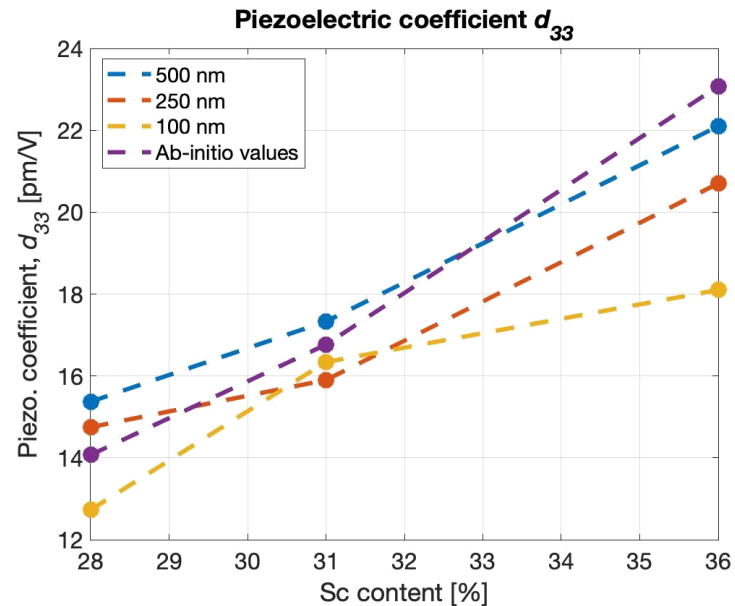
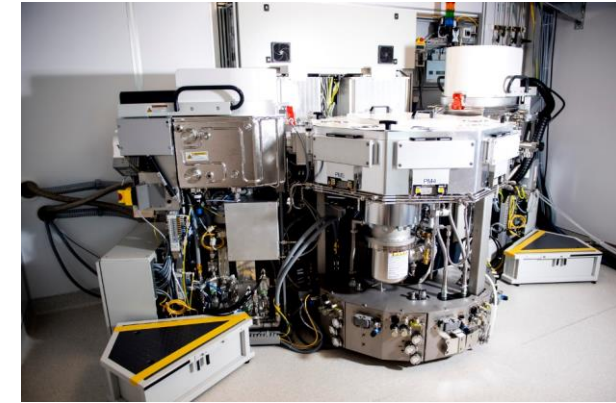
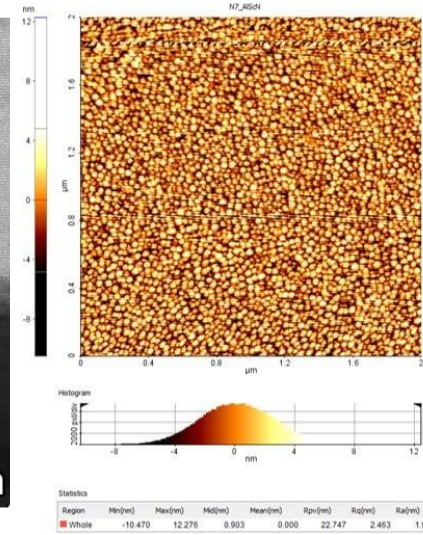
Sc-Doped AlN Material Platform for the 6G Spectrum



TEM image of $\text{Al}_{69}\text{Sc}_{31}\text{N}$ film deposited on top of Si+Ti+Pt layer stack



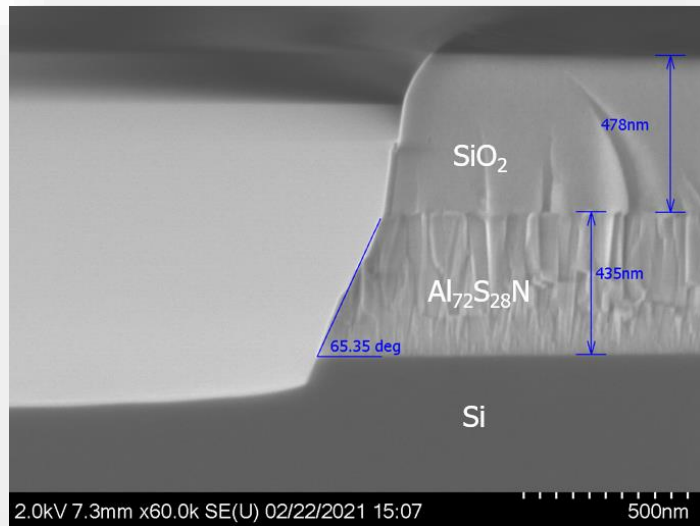
TEM image of $\text{Al}_{69}\text{Sc}_{31}\text{N}$ -Pt interface showing absence of a "dead layer"



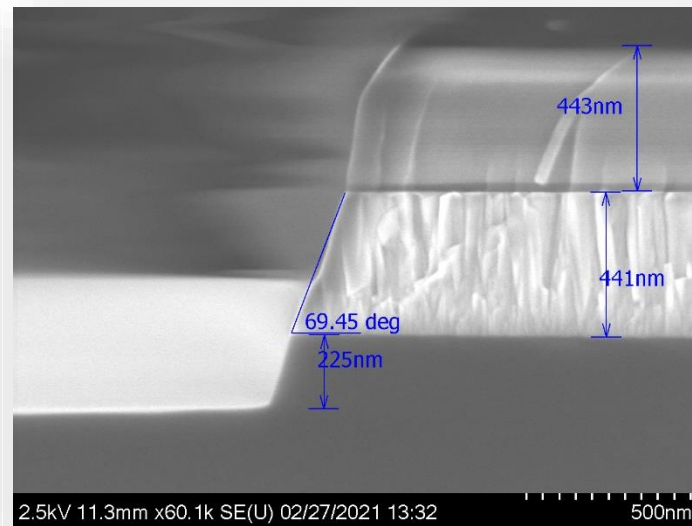
| Property | Metric | Best Measurements | Range of Measured Data |
|-----------------------|--|------------------------------|------------------------------|
| Material quality | XRD full-width-half-maximum with >90% single phase | 1.43° | 1.43° - 2.6° |
| | Surface Roughness | 0.9 nm | 0.9 - 2.07 nm |
| | Film Thickness Range | 101 - 700 nm | 101- 700 nm |
| Composition | Film stress range | 25 MPa | -309 - 414 MPa |
| | Doping value achieved | 20% - 37% | 20% - 37% |
| | Through-thickness composition variation | 0.5% | 0.5% - 2.2% |
| Electrical Properties | Lateral film composition deviation per 100 mm | 0.78% | 0.78% - 3.55% |
| | Dielectric constant | 14 | 14 - 22.3 |
| | Piezoelectric constant ($\epsilon_{31,f}$) | -2.2 C/m² | -1.4 - -2.2 C/m ² |
| | Remnant polarization | 171 μC/cm² | 90 -171 μC/cm ² |
| | Coercive field | 3.38 MV/cm | 3.38 - 5.43 MV/cm |
| | Polarization switching speed | 0.8 μs | 0.8 - 6 μs |
| | Tan δ values | 0.016 @ 5kHz | 0.016 - 0.049 |

Dry etch of AlScN

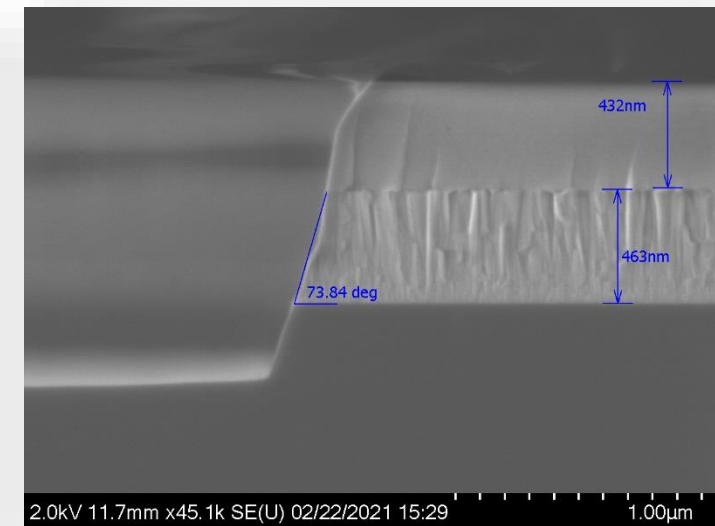
Bias Power= 200 W: $\angle \approx 65$ deg.



Bias Power= 300 W: $\angle \approx 69$ deg.



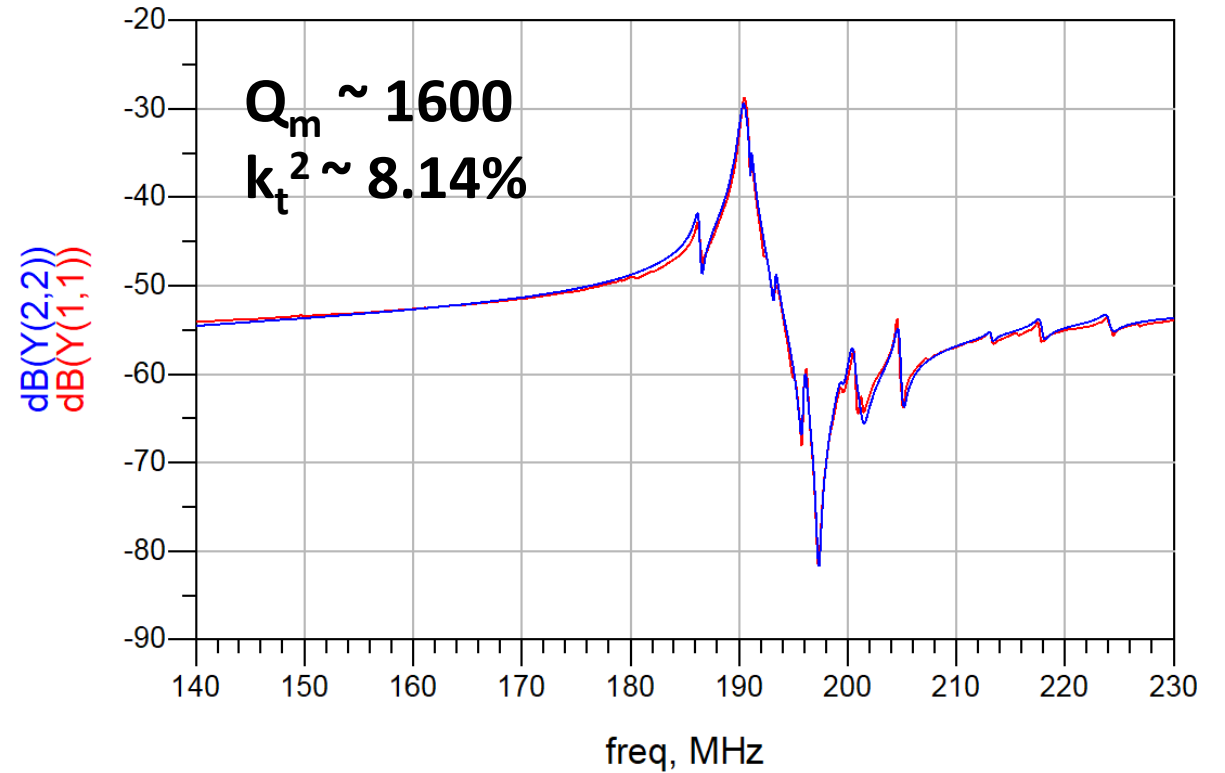
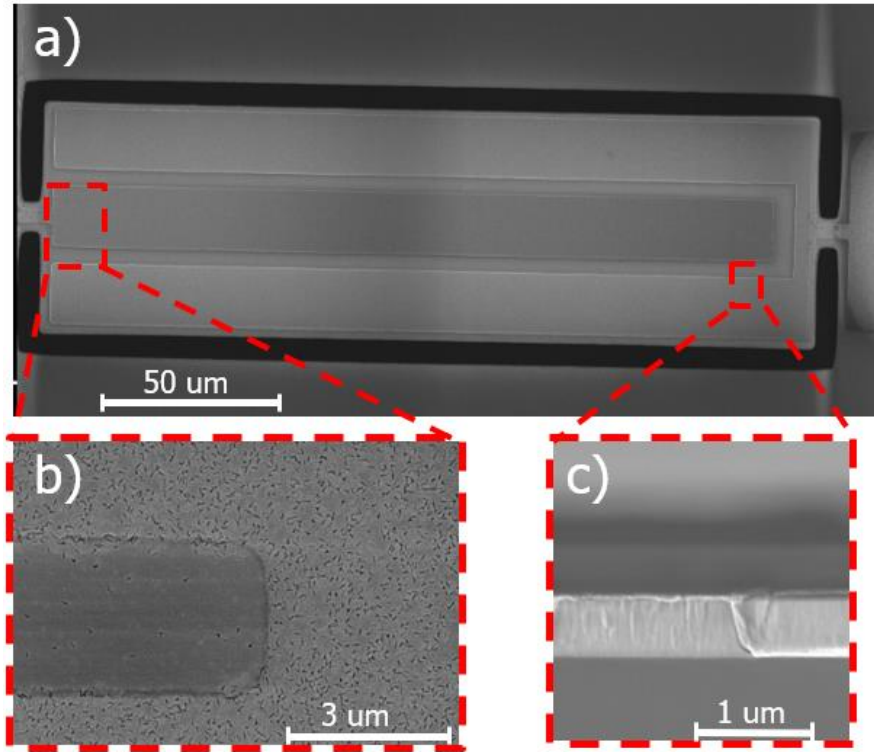
Bias Power= 400 W: $\angle \approx 74$ deg.



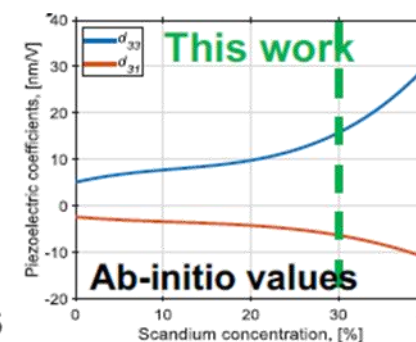
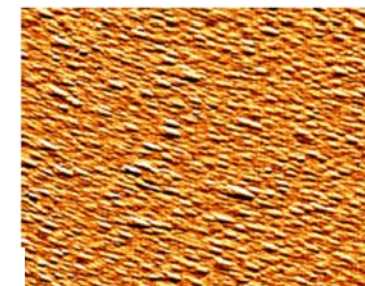
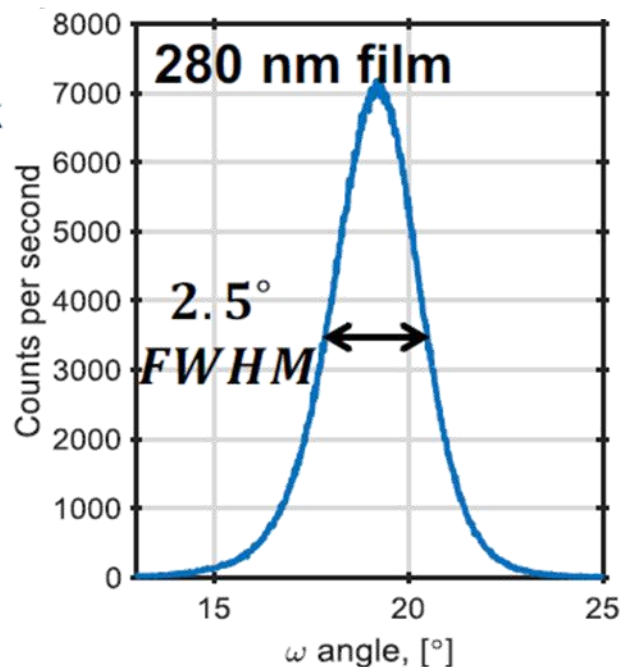
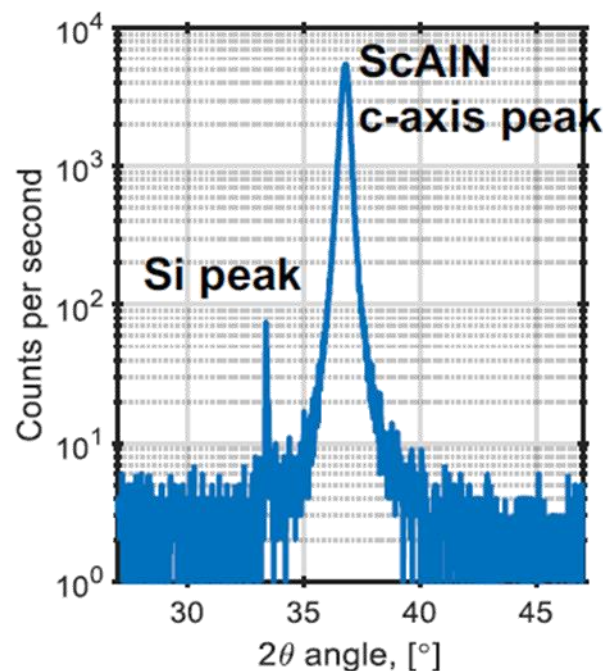
| Parameter | Value |
|---------------------------|----------|
| ICP Power | 700 W |
| RF Bias Power | 200-400W |
| Cl ₂ Gas flow | 10 sccm |
| BCl ₂ Gas flow | 6 sccm |
| Ar Gas flow | 28 sccm |
| Chamber Pressure | 10 mT |

- Low Temperature SiO₂ is used as a hard mask and can be removed via wet etch in BOE or dry etch in Ar/CF₄/CHF₃/H₂ gas mixture.
- Etch rates: Al₇₂Sc₂₈N = 140 nm/min,
SiO₂ = 120 nm/min
- Sidewall angle ≈ 74 deg.

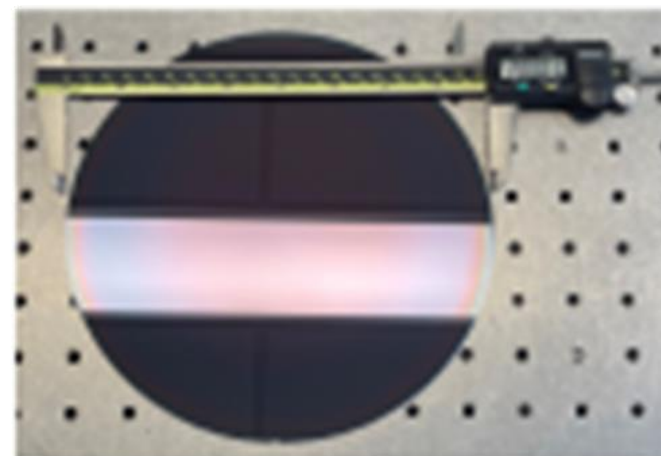
28% Sc-doped AlN Contour Mode Resonators for Low 6G Spectrum



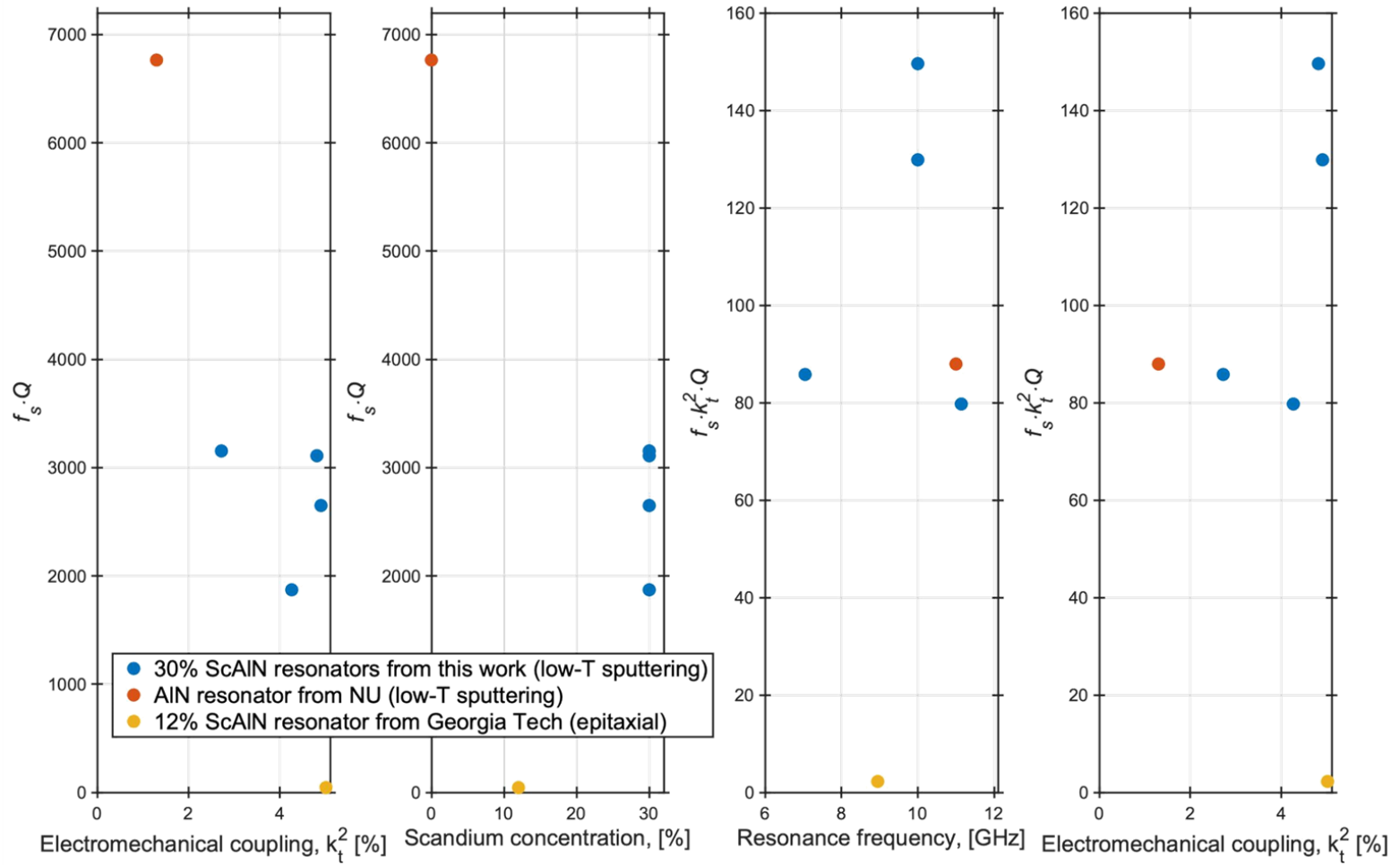
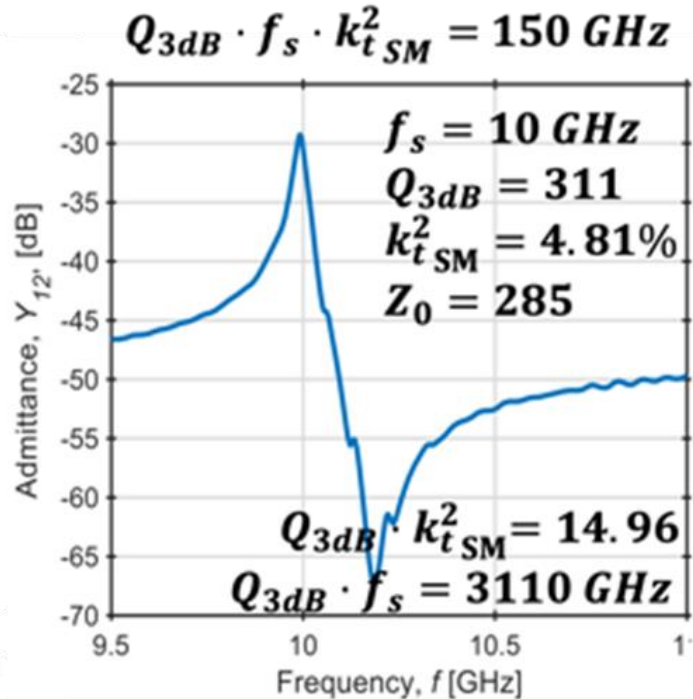
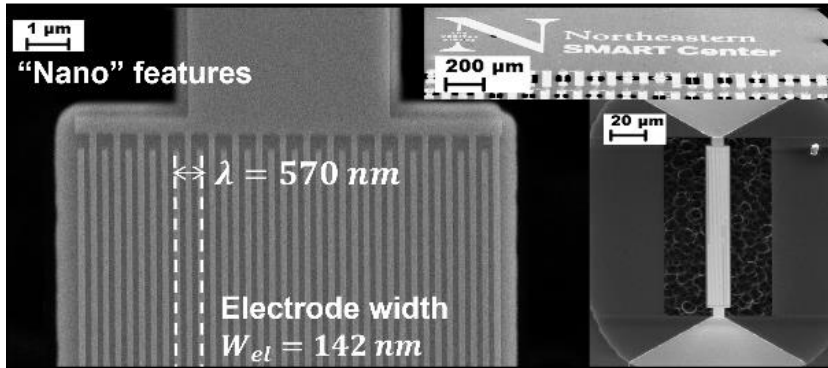
Films from 300 mm AlSc₃₀N alloy sputtering target



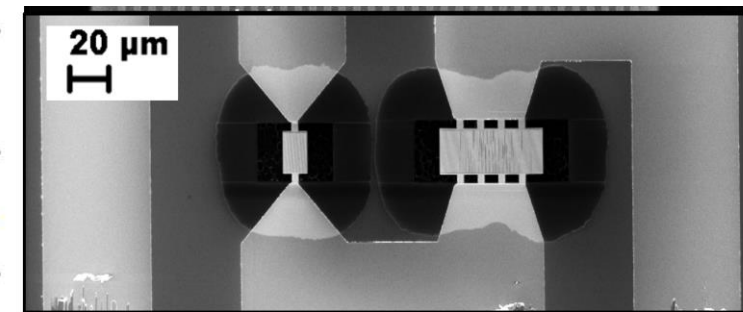
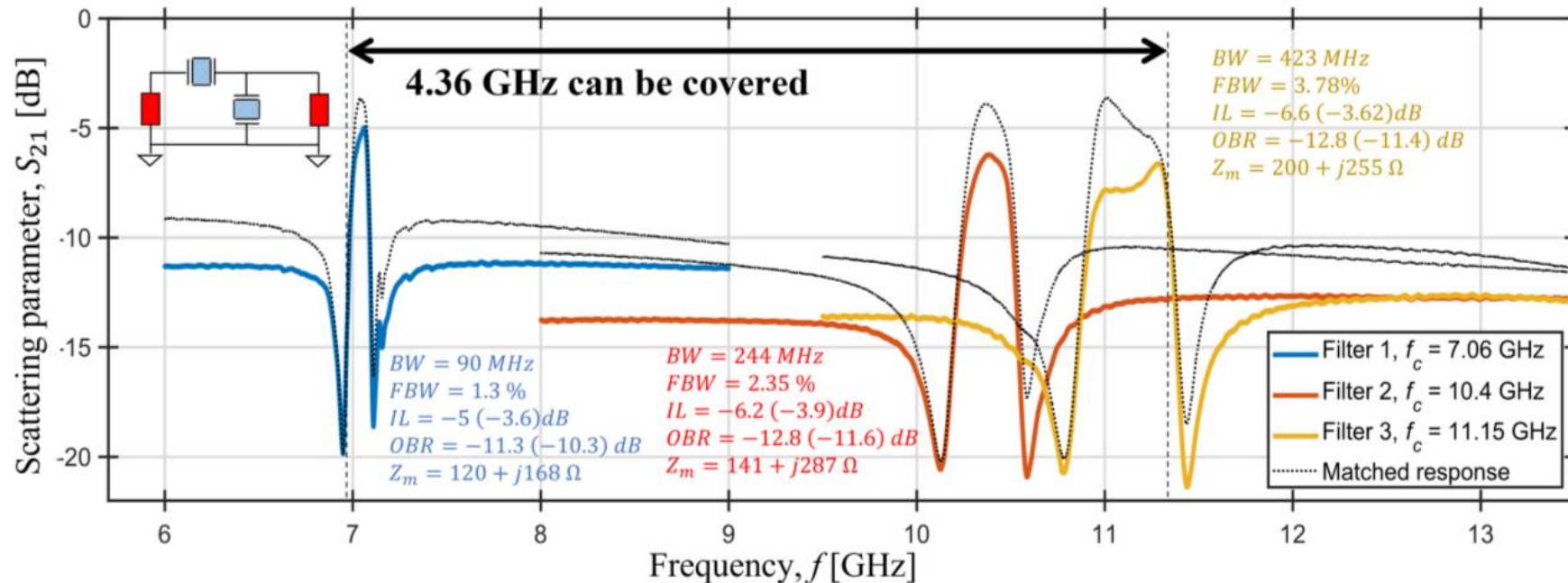
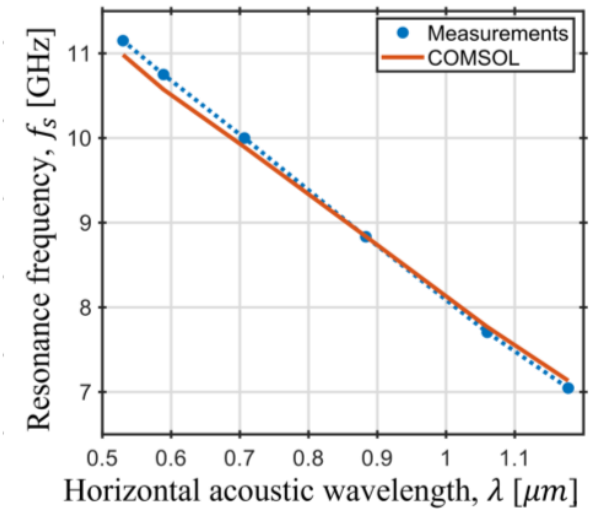
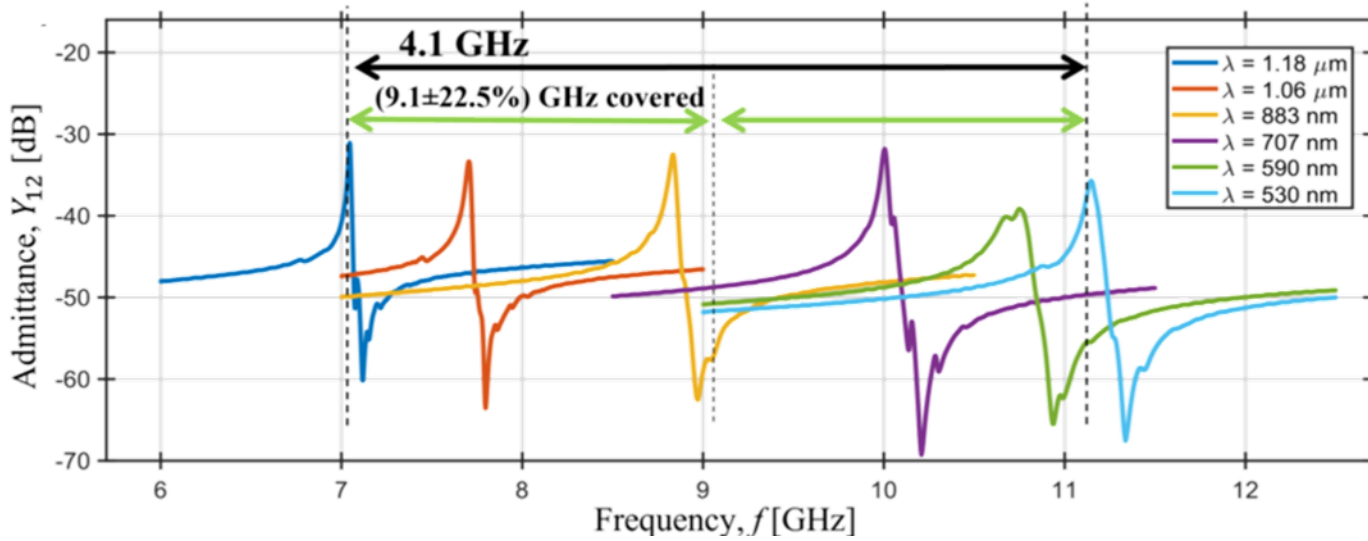
| Parameter | Value |
|--------------------------|---------|
| Power | 5 kW |
| RF Bias Power | 10 W |
| N ₂ Gas flow | 30 sccm |
| Ar ₂ Gas flow | 0 sccm |
| Temperature | 300 °C |
| Chuck height | 20 mm |



30% AlScN CLMRs - Highest figure of merit SHF Acoustic Resonator



Single-chip Multi-Band SHF AlSc₃₀N Filters



Acknowledgement

Research Faculty:

- Prof. Zhenyun Qian

Research Scientists:

- Dr. Cristian Cassella
- Dr. Luca Colombo

Postdocs:

- Dr. Pietro Simeoni
- Dr. William Zhu
- Dr. Tao Wu

Ph.D. Students:

- Yu Hui
- Zhenyun Qian
- Guofeng Chen
- Gwendolyn Hummel
- Ryan Sungho Kang
- Vageeswar Rajaram
- Yao Yu
- Bernard Herrera Sokup
- Michele Pirro
- Sila Deniz Calisgan
- Flavius Pop
- Giuseppe Michetti
- Mika Assylbekova
- Antea Risso
- Hussein Hussein
- Gabriel Giribaldi
- Farah Ben Ayed

